Metallurgy and materials
Metalurgia e materiais

Three-dimensional reconstruction of compacted graphite in vermicular cast iron by manual serial sectioning

http://dx.doi.org/10.1590/0370-44672014680120

Fernando Almeida Cerqueira
Aluno de graduação -
Universidade de São Paulo - Escola Politécnica,
Departamento de Engenharia Metalúrgica
e de Materiais -
São Paulo – São Paulo – Brazil
facerq@gmail.com

Arthur Seiji Nishikawa
Aluno de pós-graduação -
Universidade de São Paulo - Escola Politécnica,
Departamento de Engenharia Metalúrgica
e de Materiais -
São Paulo – São Paulo – Brazil
arthur.nishikawa@usp.br

Wilson Luiz Guesser
Pesquisador -
Fundição Tupy - Pesquisa e Desenvolvimento
Joinvile – Santa Catarina - Brazil
wguesser@tupy.com.br

Cesar Roberto de Farias Azevedo
Professor -
Universidade de São Paulo - Escola Politécnica,
Departamento de Engenharia Metalúrgica
e de Materiais -
São Paulo – São Paulo – Brazil
c.azevedo@usp.br

Abstract

Microstructural characterization is an important tool to optimize the properties of engineering materials. Metallography is a common technique, but it provides two-dimensional images from (sometimes complex) three-dimensional microstructures. Three-dimensional reconstruction of microstructures provides more precise information on the morphologies of the material microconstituents, providing more accurate control over their physical and mechanical properties. The main barrier for the dissemination of this technique is the extensive time dispended to obtain a record of innumerous metallographic polished planes and the 3D image reconstruction procedure. The present work shows a practical example of three-dimensional reconstruction of the graphite phase in a compacted graphite cast iron executed by "manual" technique and using optical microscopy.

Keywords: Compacted graphite iron, graphite morphology, three-dimensional reconstruction.

1. Introduction

Since the appearance of metallography in 1863, the information obtained from viewing images of the polished and etched cross-sections of metals led to the development of metallurgical engineering. The observation of these two dimensional microstructural images allowed to correlate the microstructure with the manufacturing and materials properties. Additionally, it allowed the investigations of the mechanisms of nucleation and growth during phase transformation and the properties of the material, in spite of the limitations of the metallographic technique, due to the three-dimensional aspect of the microstructures (Kral *et al*., 2000, Tewari and Gokhale, 2001, Singh and Gokhale, 2005, Holm and Duxbury, 2006, Spowart, 2006, Denis *et al*., 2008, Azevedo and Marques, 2010). Hillert (1962), developed the technique of serial sectioning to investigate a single colony of pearlite. He produced 242 metallographic sections through serial polishing and etching and produced a moving picture film to understand the three-dimensional morphology of the pearlite. He concluded that the formation of pearlite colonies was the result of the interlacing of ferrite and cementite single crystals, contrary to a theory proposed by Hull and Mehl (1942) that the pearlite was formed by the successive nucleation of lamellae of cementite and ferrite. De Hoff, 1983, assessed the state of the art of the serial sectioning technique to investigate 3D microstructures, highlighting the importance of this technique to obtain more detailed

information on the morphology of precipitates. Hull *et al.* (1991) studied the volumetric distribution of the former β grain in near-α IMI 629 titanium alloy using a serial sectioning technique associated with a computational method to reconstruct the microstructure in 3 D. The results showed the β grain surfaces with a step-like morphology, indicating that 3D reconstruction required a higher resolution in terms of numbers of metallographic sections and more sophisticated software for the reconstruction of 3D microstructure.

Mangan *et al.* (1997) obtained 3D images of cementite Widmanstätten platelets of a Fe-12.3%Mn-0.8%C steel. These results were coupled with electron backscatter diffraction (EBSD) results in order to get a 3D microstructural reconstruction with crystallographic orientation-relationship information. The authors were able to conclude that the cementite platelets established a Pitsch orientation-relationship with the austenitic matrix. Kral and Spanos (1999) showed that the pro-eutectoid cementite of steels did not nucleate inside the austenitic grains, but along the previous austenitic grain boundaries. They also observed that the sub-grains acted as barriers to the growth of pro-eutectoid cementite rather than potential nucleation sites. Between 2002 and 2008, more investigators used serial metallography to reconstruct 3D microstructures (Hung *et al.*, 2002, Kuijpers *et al.*, 2002, Wu. 2006, Sidhu and Chawla, 2003, Dinnis *et al.*, 2005, Dudek and Chawla, 2008). Graef *et al.* (2006) reviewed the results of Hillert (1962) using more modern techniques for 3D reconstruction. They observed more clearly the branching of the cementite single crystal and the resulting formation of cementite lamellae in a single pearlite colony. In Brazil, Contieri *et al.* (2008) used the serial sectioning technique associated with scanning electron microscopy to investigate the 3D morphology of the ternary eutectic of an Nb-Al-Ni alloy. In conventional metallography, the ternary eutectic (Al_3Nb+Nb2Al+AlNbNi) seemed to be semi-continuous, but the three-dimensional reconstruction made it clear that these phases were continuous.

However, the manual serial sectioning technique requires considerable effort for sample preparation. In this sense, the serial sectioning via dual-beam focused ion beam-scanning electron microscope (FIB-SEM) was able to more efficiently and accurately perform the documentation of the various metallographic plans. Besides, it allowed obtaining high-resolution images associated with other analytical results, such as crystallographic orientation (EBSD) and chemical microanalysis (Rowenhorst *et al.*, 2006, Lewis and Geltmacher, 2006, Lasagni *et al*, 2007, Lee *et al.*, 2007, Zaefferer, 2007). Velichko *et al.* (Velichko *et al.*, 2007) used serial sectioning via FIB-SEM to investigate the various morphologies of graphite in cast irons. They demonstrated after 3D reconstruction of the microstructure the role of second phase particles and non-metallic inclusions on the nucleation of graphite. Wang *et al.* (2010) used the serial sectioning via FIB-SEM technique to investigate the mechanism of pearlite spheroidization. The authors stated that only the 3D reconstruction allowed a better visualization of the microstructural and crystallographic evolution of the cementite spheroidization. When compared to the deep etching technique for SEM analysis, the 3D reconstruction technique allowed the 3D visualization of each one of the various micro-constituents, permitting the rotation of each one of these elements for better morphological examination. Additionally, the reconstructed 3D microstructures can be exported to a finite element analysis (FEA) software to simulate the mechanical and physical properties of 3D microstructures. Lee *et al.* (2006) used a 3D high-resolution reconstruction to investigate the interconnectivity of microporosity in a magnesium alloy. They applied finite element analysis on the resulting 3D microstructure to calculate the stress concentration factors in the matrix adjacent to the microporosities, allowing the identification of stress concentrators in the microstructure.

The objective of the present work is to investigate the morphology of compacted graphite in vermicular cast iron using manual serial sectioning and the three-dimensional reconstruction technique.

2. Materials and methods

A vermicular cast iron with pearlitic matrix was analyzed. The metallographic sections were prepared according to standard procedures (silicon carbide abrasive paper grinding, diamond grit polishing and unetched samples). Final polishing was performed using 0.06 µm colloidal silica mixed with a small quantity of 0.3 µm alumina gel. The polished surfaces were not etched to observe the morphologies of graphite. The images were obtained using an Olympus light microscope under 2 different magnifications (100 x and 200 x). The average spacing between each serial image defines the resolution of the three-dimensional virtual object. For example, Kral *et al.* (2000) obtained more than 200 sections (images) for the 3D reconstruction of cementite during the decomposition of austenite. The alignment of these images in translational and rotational terms was obtained by using a pair of Vickers microhardness indentation marks (Zwick & Co microhardness testing machine) as references. The thickness of the material in each step of the serial sectioning was calculated by measuring the variation in the dimensions of the indentations marks. The metallographic procedure conditions must be reproducible to well define the contours of the graphite, without the presence of any metallographic artifacts. The present work used 96 metallographic sections for the three-dimensional reconstruction of the microstructure with an average spacing between each serial image around 0.8 µ. Image acquisition was performed in an Olympus BX60M optical microscope coupled with 3.2 megapixels Micrometrics 318CU digital a camera. Micrometrics Premium SE version 2.8 software was used to capture images, with the dimensions of 2048 x 1536 pixels, 96 dpi resolution (in both dimensions) in colored bitmap mode with intensity of 24 bits. The various metallographic sections were assumed to be parallel. The metallographic images were treated with Java Image J free version 1.40 software. 3D reconstruction was performed using Reconstruct 1.1.0.0 free software (developed by Neural Systems Laboratory at Boston University). The Boissonnat surface was chosen for 3D reconstruction of the surfaces of the graphite particles. The microhardness indentation marks were used to align the images before stacking them (see figure 1).

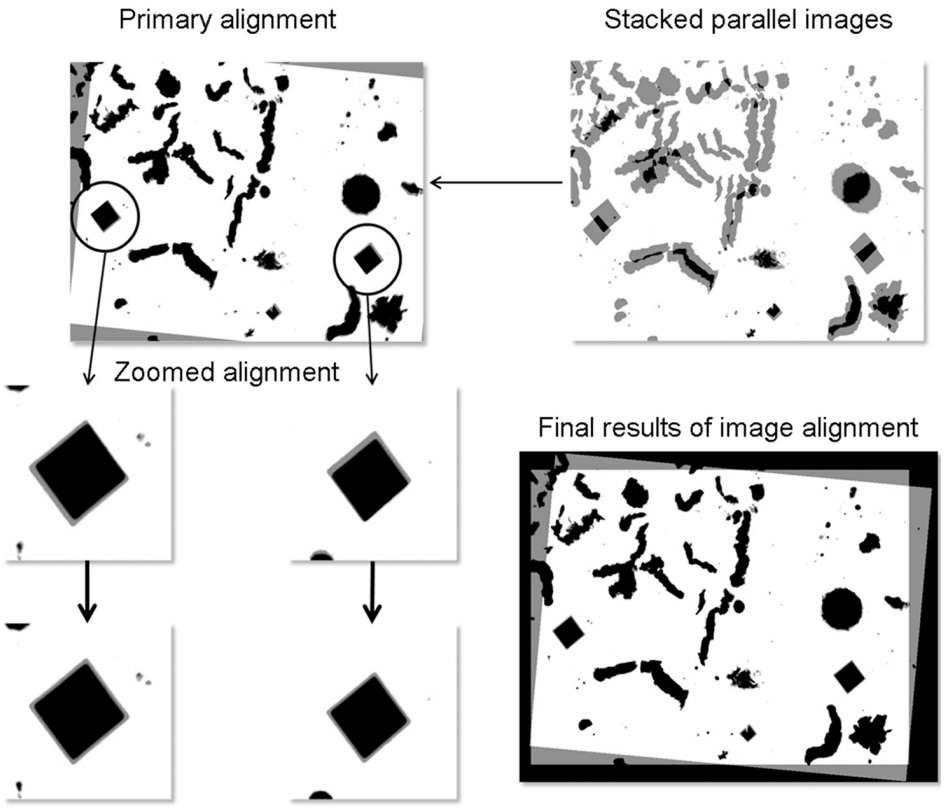

Figure 1:
Scheme showing
the alignment of parallel images
using a pair of Vickers indentations marks

3. Results

Figures 2a to 2b shows the reconstructed 3D morphology of the compacted graphite. The different colors are used to show units of interconnected graphite within the reconstructed volume. The results show that there is a wide variation in the morphology of graphite, with the presence of few graphite nodules and also other morphologies presenting a transition from nodular to compacted graphite.

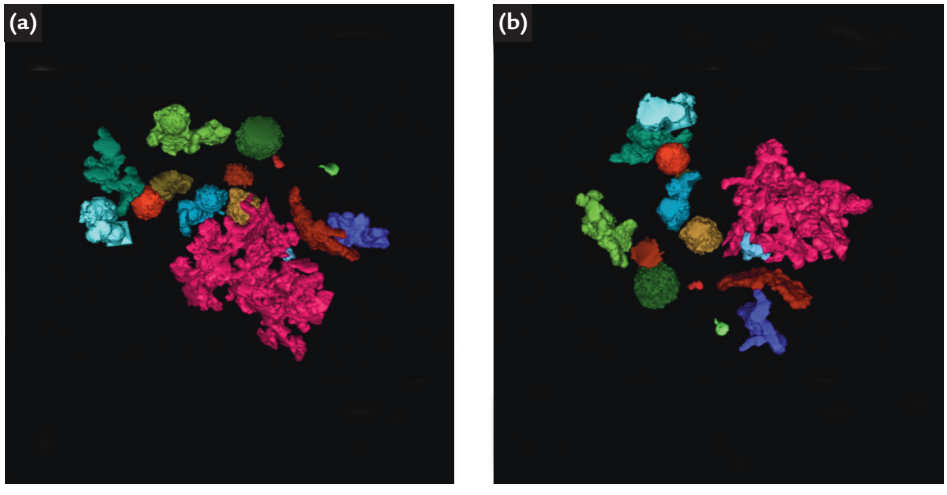

Figure 2
3D reconstruction
of the compacted graphite (100X).

The 3D reconstruction provides more accurate information on the morphologies of graphite when compared to conventional metallography (see Figures 3a to 3d). Some of the graphite nodules on conventional metallography were seen after 3D reconstruction to be interconnected, forming compacted graphite (see Figures 3a and 3c). Even a perfect nodule on conventional metallography (see Figure 3b) shows after 3D reconstruction a characteristic bulge, typical of <a> direction growth of the hexagonal crystal (see Figure 3d). Another feature of the 3D reconstruction is to show that units of graphite apparently disconnected in the conventional metallographic examination can be interconnected in the space, forming a single crystal of graphite. A metallographic section of Figure 4a distant and isolated vermicular graphite structures in purple, but the 3D reconstruction showed that these purple units are interconnected in the space, forming a single crystal (see Figure 4b). In the same picture (figure A), relatively nearby graphite structures were not connected in the reconstructed volume. It is likely that some interconnectivity of the graphite structures might happen outside the reconstructed volume. Finally, it was also possible to observe the presence of small "star-shaped" non-metallic inclusions (see Figures 5-a and 5-b). This morphology inclusion would hardly be observed in the conventional metallographic examination.

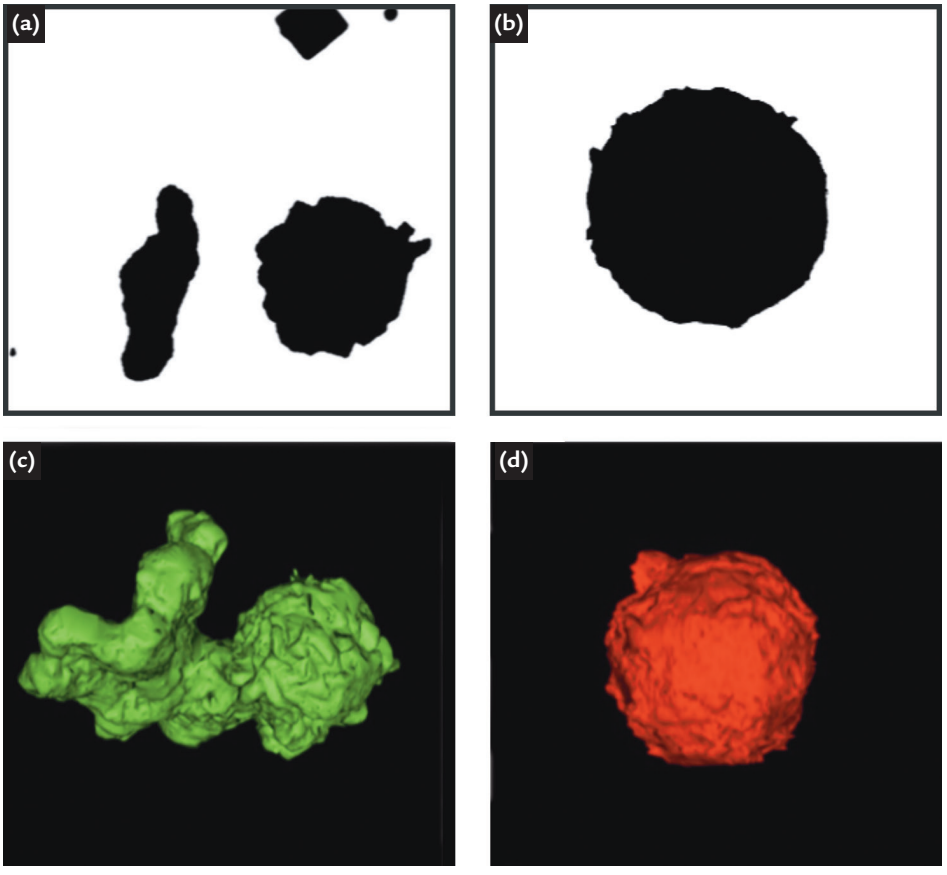

Figure 3
Comparison of conventional metallography results of the same area (a) and (b) with the 3D reconstruction technique results in terms of graphite morphology (c) and (d) (200X).

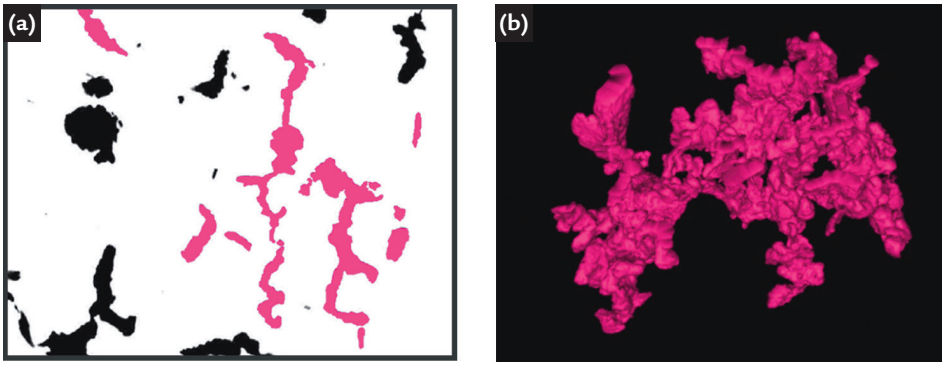

Figure 4
Comparison of conventional metallography results (a) with the 3D reconstruction technique results (b) in terms of graphite interconnectivity morphology (100x).

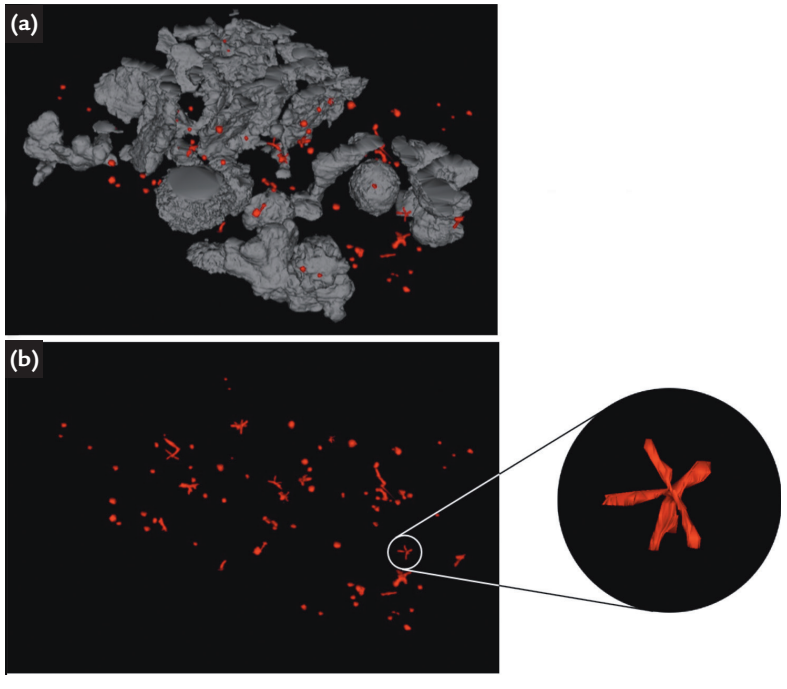

Figure 5
Presence of small "star-shaped" non-metallic inclusions (a) and (b).

4. Discussion

The 3D reconstruction of graphite in vermicular cast iron confirms the connectivity of the graphite phase in a greater scale than observed in the metallographic tests (see Figures 2 to 4). However, this graphite continuity does not come in the form of plates, as in gray cast irons. The morphology of compacted graphite in vermicular cast iron can be approximated to the form of a hand with the thick plates of graphite in the form of a palm connected to the cylindrical graphite shapes resembling fingers. This continuous microstructure of the graphite is similar to what occurs in gray cast iron, in which the growth of the eutectic cell takes place by the partial cooperative growth with the austenite phase. This morphology of compacted graphite has profound implications in the physical and mechanical properties of vermicular cast iron: the crack growth in the vermicular cast iron also requires a rupture of the austenite matrix located between the "fingers-shaped" graphite, so that the crack growth within the eutectic cell in vermicular cast iron requires higher energy consumption than in the fracture of the gray cast iron. As a consequence, the fractographic observation of grey cast iron shows a predominance of plate-like graphite fracture, while in vermicular cast iron, an appreciable amount of ferrous matrix ductile fracture is observed. Vermicular cast iron has been replacing the grey cast irons in applications with requirements of greater mechanical strength and ductility without significant loss in thermal conductivity (Guesser, 2002). The presence of graphite nodules in microstructure of vermicular cast irons has always been much discussed (Fuoco, 1989, Fuoco et al., 1989, Fuoco, 2013,). Samples with a deep attack along with the conventional metallographic observation suggest the presence of graphite nodules, but 3D reconstructions allowing the observation of graphite nodules presenting lamellar ramification can be observed, suggesting the early growth of compact graphite. The 3D viewing confirmed – for the observed volume – that nodules of graphite and compacted graphite might be in some cases part of the same hexagonal graphite crystal, with growths along the <c> direction (nodule formation) and along the <a> direction (lamella formation) (see Figure 3c). In addition, in Figure 3d a graphite nodule with an interrupted growth along the <a> direction is observed. Additionally 3 D microstructural reconstruction is more efficient in dealing with the interconnectivity of the graphite microstructure (see Figures 4a and 4b). Finally, an interesting result of the 3D reconstruction was the identification of the "star-shaped" non-metallic inclusions in the material (see Figure 5-b), whose observation is rare in literature (Fuoco, 2013). Further work will simulate the thermal conductivity of the vermicular cast iron using 3D reconstruction microstructure coupled with FEA.

5. Conclusions

• The 3D reconstruction is a more efficient tool to investigate the continuity of the compacted graphite microstructure.

• The 3D reconstruction showed the presence of “star-shaped non-metallic inclusions”.

6. References

AZEVEDO C.R.F., MARQUES, E. R. Three-dimensional analysis of fracture, corrosion and wear surfaces. ***Engineering Failure Analysis***, v.17, n.1, p. 286–300, 2010.

CONTIERI, R. J. et al. Growth and three-dimensional analysis of a Nb–Al–Ni ternary eutectic. ***Materials Characterization,*** v. 59, n. 6, p. 693-699, 2008.

DE HOFF, R. T. Quantitative serial sectioning analysis: preview. ***Journal of Microscopy***, v. 131, n. 3, p. 259-263, 1983.

DENIS, E. P. et al. 3D complex shape characterization by statistical analysis: application to aluminium alloys. ***Materials Characterization,*** v. 59, n. 3, p. 338-343, 2008.

DINNIS, C. M. et al. Three-dimensional analysis of eutectic grains in hypoeutectic Al–Si alloys. ***Materials Science and Engineering:*** A, v. 392, n. 1-2, p. 440-448, 2005.

DUDEK, M. A., CHAWLA, N. Three-dimensional (3D) microstructure visualization of LaSn3 intermetallics in a novel Sn-rich rare-earth-containing solder. ***Materials Characterization,*** v. 59, n. 9, p. 1364-1368, 2008.

FUOCO, R., ALBERTIN, E., AZEVEDO, C. R. F. Efeito do carbono equivalente na morfologia da grafita e na microestrutura de ferros fundidos vermiculares. ***Metalurgia ABM***, São Paulo, v. 45, n.382, p. 914-921, 1989.

FUOCO, R. ***Processo de produção de ferros fundidos com grafita vermicular através do tratamento com magnésio e alumínio.*** Escola Politécnica da Universidade de São Paulo, 1989. (Disssertação de Mestrado).

FUOCO, R. ***Personal communication on March.*** 2013.

GRAEF, M. D. et al. A modern 3-D view of an “old” pearlite colony. ***JOM***, v. 58, n. 12, p. 25-28, 2006.

GUESSER, L. Ferro fundido com grafita compacta. ***Metalurgia e Materiais,*** p. 403-405, junho 2002.

HILLERT, M. The formation of pearlite. In: Zackay, V. F., Aaronson, H. I.(Eds.). ***Decomposition of Austenite by Diffusional Processes***. Interscience Publishers, Inc / John Wiley & Sons, 1962. 691 p.

HOLM, E. A., DUXBURY, P. M. Three-dimensional materials science. ***Scripta Materialia,*** v. 54, n. 6, p. 1035-1040, 2006.

HULL, D. et al. Titanium prior-beta grain volume distribution by quantitative serial sectioning techniques. ***Materials Characterization,*** v. 26, n. 2, p. 63-71,1991.

HULL, F. C., MEHL, R. F. The structure of pearlite. ***Transacions of the American Institute for Metals,*** v. 30, n. 6, p. 381-424, 1942.

HUNG, C.-Y. et al. Three-dimensional observations of proeutectoid cementite precipitates at short isothermal transformation times. ***Acta Materialia,*** v. 50, n. 15, p. 3781-3788, 2002.

KRAL, M. V., SPANOS, G. Three-dimensional analysis of proeutectoid cementite precipitates. ***Acta Materialia,*** v. 47, n. 2, p. 711-724, 1999.

KRAL, M. V. et al. Three-dimensional analysis of microstructures. ***Materials Characterization,*** v. 45, n. 1, p. 17-23, 2000.

KUIJPERS, N. C. et al. Quantification of the evolution of the 3D intermetallic structure in a 6005A aluminium alloy during a homogenisation treatment, ***Materials Characterization,*** v. 48, n. 5, p. 379-392, 2002.

LASAGNI, F. et al. Three-dimensional characterization of "as-cast" and solution-treated AlSi12(Sr) alloys by high-resolution FIB tomography, ***Acta Materialia,*** v. 55, n. 11, p. 3875-3882, 2007.

LEE, S. B. et al. Three-dimensional microstructure reconstruction using FIB-OIM, ***Materials Science Forum,*** v. 558-559, p. 915-920, 2007.

LEE, S. G. et al. Reconstruction and visualization of complex 3D pore morphologies in a high-pressure die-cast magnesium alloy, ***Materials Science and Engineering: A,*** v. 427, n. 1-2, p. 92-98, 2006.

LEWIS, A. C., GELTMACHER, A. B. Image-based modeling of the response of experimental 3D microstructures to mechanical loading, ***Scripta Materialia,*** v. 55, n. 1, p. 81-85, 2006.

MANGAN, M. A. et al. Three-dimensional reconstruction of Widmanstatten plates in Fe-12.3Mn-0.8C, ***Journal of Microscopy,*** v. 188, n. 1, p. 36-41, 1997.

ROWENHORST, D. J. et al. 3D Crystallographic and morphological analysis of coarse martensite: Combining EBSD and serial sectioning, ***Scripta Materialia,*** v. 55, n. 1, p. 11-16, 2006.

SIDHU, R. S. CHAWLA, N. Three-dimensional (3D) visualization and microstructure-based modeling of deformation in a Sn-rich solder, ***Scripta Materialia,*** v. 54, n. 9, p. 1627-1631, 2006.

SINGH, H. GOKHALE, A. M. Visualization of three-dimensional microstructures, ***Materials Characterization,*** v. 54, n. 1, p. 21-29, 2005.

SPOWART, J. E. Automated serial sectioning for 3-D analysis of microstructures, ***Scripta Materialia***, v. 55, n. 1, p. 5-10, 2006.

TEWARI, A. GOKHALE, A. M. Estimation of three-dimensional grain size distribution from microstructural serial sections, ***Materials Characterization,*** v. 46, n. 4, p. 329-335, , 2001.

VELICHKO, A. et al. 3D characterization of graphite morphologies in cast iron, ***Advanced Engineering Materials,*** v. 9, n. 1-2, p. 39-45, 2007.

WANG, Y.-T. et al. Quantitative three-dimensional characterization of pearlite spheroidization, ***Acta Materialia,*** v. 58, n. 14, p. 4849-4858, 2010.

WU, K. M. Three-dimensional analysis of acicular ferrite in a low-carbon steel containing titanium, ***Scripta Materialia,*** v. 54, n. 4, p. 569-574, 2006.

ZAEFFERER, S. et al. 3D-orientation microscopy in a FIB SEM: a new dimension of microstructure characterization, ***Microscopy and Microanalysis,*** v. 13, n. S02, 2007.

Received: 01 July 2014 - Accepted: 15 December 2015.